Materials Science and Engineering B 117 (2005) 53–61

www.elsevier.com/locate/mseb

Finite element analysis-based design of a fluid-flow control nano-valve

M. Grujicic[a,*], G. Cao[a], B. Pandurangan[a], W.N. Roy[b]

[a] *Department of Mechanical Engineering, Program in Materials Science and Engineering, Clemson University, Clemson, SC 29634, USA*
[b] *Army Research Laboratory, Processing and Properties Branch, Aberdeen, Proving Ground, MD 21005-5069, USA*

Received 24 June 2004; received in revised form 17 October 2004; accepted 20 October 2004

Abstract

A finite element method-based procedure is developed for the design of molecularly functionalized nano-size devices. The procedure is aimed at the single-walled carbon nano-tubes (SWCNTs) used in the construction of such nano-devices and utilizes spatially varying nodal forces to represent electrostatic interactions between the charged groups of the functionalizing molecules. The procedure is next applied to the design of a fluid-flow control nano-valve. The results obtained suggest that the finite element-based procedure yields the results, which are very similar to their molecular modeling counterparts for small-size nano-valves, for which both types of analyses are feasible. The procedure is finally applied to optimize the design of a larger-size nano-valve, for which the molecular modeling approach is not practical.

Keywords: Single-walled carbon nano-tubes; Nano-devices; Nano-technology

1. Introduction

In the last several years, considerable effort has been invested into studying functionalized (typically silicon-based) cantilever nano-beams e.g. [1,2]. Such nano-beams have one face covered (functionalized) with self-assembled or chemically bonded molecules of various types and can deflect by themselves due to differences in the surface stress between the functionalized and non-functionalized faces. In a recent paper, Solares et al. [3] proposed the design of a fluid-flow control nano-valve based on a silicon nano-beam actuator functionalized with a covalently bonded monolayer of acrylic acid molecules, which can allow or stop the flow through a fluid conduit, a single-walled carbon nano-tube (SWCNT). The "*on/off*" switching of the nano-valve is controlled by the pH of its environment. That is, changes in the pH affect the charges of the bonded molecules and, thus, control the magnitude of the inter-molecular electrostatic forces.

Solares et al. [3] argued that as molecular modeling is moving from being primarily a tool for studying materials properties to an alternative approach for analyzing the performance of devices, it is becoming computationally more and more demanding and, often, impractical. This is caused by the fact that the size of the computational problem generally increases as N^2, where N is the number of particles in the system being studied. This problem is particularly aggravated by the presence of electrostatic interactions between the charged molecules used for nano-beam functionalization because of the following two main reasons: (a) the geometry of nano-devices is generally not periodic so that efficient electrostatic lattice-summation methods (e.g. the Ewald summation method) cannot be used without introducing spurious effects due to imposition of the periodic boundary conditions and (b) the use of radial cut-off radii or splines to handle the long-range interactions can underestimate the electrostatic energy by as much as an order of magnitude for the nanometer-size devices. There is an additional problem associated with the use of molecular modeling methods for simulation of the nano-size devices. Average forces and strain energies used to judge the attainment of equilibrium may not be very reliable in a computational system containing a large number of particles, since they may allow large residual forces to be present in a small region, while the average

* Corresponding author. Tel.: +1 864 656 5639; fax: +1 864 656 4435.
E-mail address: mica.grujicic@ces.clemson.edu (M. Grujicic).

0921-5107/$ – see front matter © 2004 Elsevier B.V. All rights reserved.
doi:10.1016/j.mseb.2004.10.020

force is quite small implying an equilibrium state of the system.

Nevertheless, to obtain a more accurate design of a nano-device, it is critical to include as much molecular level details as possible. As pointed out above, on the other hand, it is often impractical or impossible to carry out all design and analysis steps at the molecular level. To achieve a compromise, Solares et al. [3] proposed a hybrid method, which combines molecular simulations with the classical engineering design. Specifically, molecular simulations are used to determine elastic and electrostatic properties of the individual components of a nano-device, which are then used, within a classical engineering design framework, to carry out an analysis of the functionality, design, and optimization of the nano-device.

The objective of the present work is to extend the hybrid method proposed by Solares et al. [3] and apply it to the design of a fluid-control valve described above. Specifically, the method of Solares et al. [3] fails to include the interactions between different device components (primarily the interactions between the cantilever nano-beam and the SWCNT) during the operation of such a nano-valve. Rather, the performances of the cantilever nano-beam and the SWCNT fluid conduit are analyzed separately and that information used to judge the functionality of the nano-device and determine its optimal geometry and dimensions. In the present work, we extend the hybrid method proposed by Solares et al. [3] by utilizing a finite element method to analyze the performance of the entire nano-valve and use the results of such analysis as a guide for optimization of the device design. In this way, the interactions between the cantilever nano-beam and the SWCNT, which are at the heart of operation of the functionalized silicon cantilever nano-beam-based nano-valve, are directly taken into account.

The organization of the paper is as follows: a brief formulation to the problem being studied is given in Section 2.1. The use of the shell theory to model the SWCNT wall within a continuum formulation is presented in Section 2.2. The development of special contact elements, which account for the van der Waals interactions between contacting surfaces is presented in Section 2.3. The procedure used to compute energy and force associated with the electrostatic interaction between the charged functionalizing molecules is explained in Section 2.4. The method employed to specify the initial internal stress in the SWCNT wall is described in Section 2.5. A brief overview of the finite element method used is given in Section 2.6. The main results obtained in the present work are presented and discussed in Section 3, while the key resulting conclusions are summarized in Section 4.

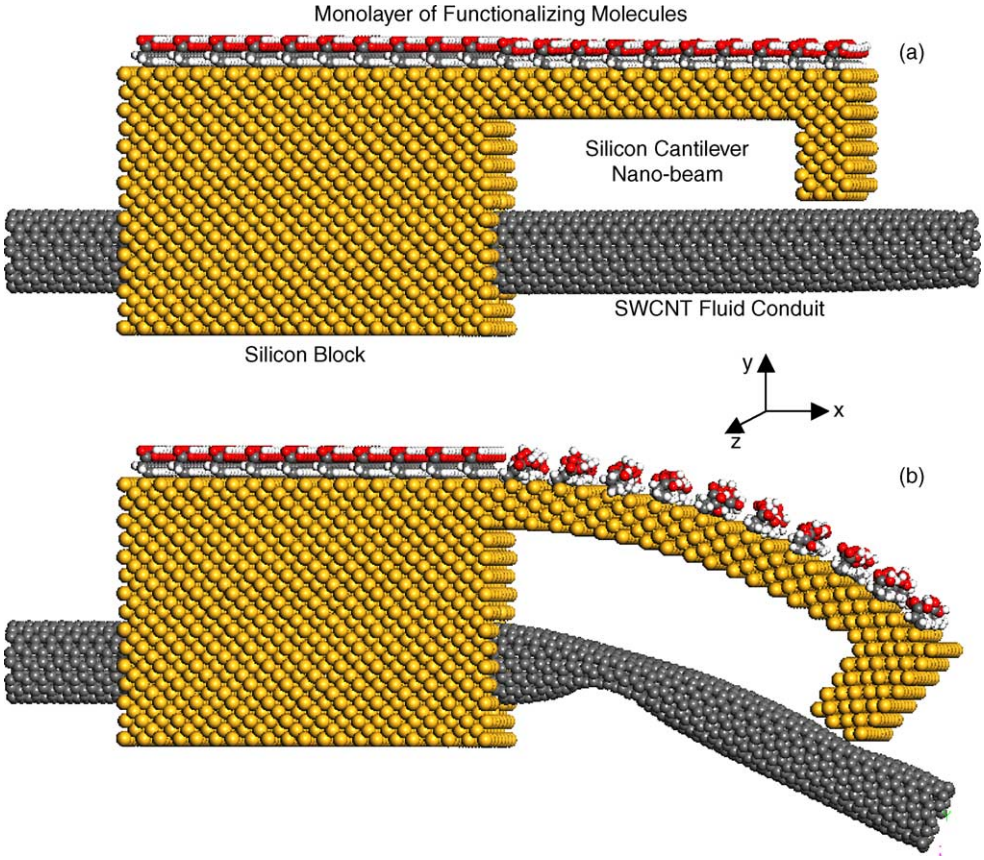

Fig. 1. Atomistic structure of the fluid-flow control nano-valve analyzed in the present work in the: (a) open and (b) closed positions.

2. Computational procedure

2.1. Problem definition

Atomistic configurations of the nano-valve in the open and closed positions are displayed in Fig. 1(a) and (b), respectively. The nano-valve consists of a silicon block with a cantilever nano-beam, where both are functionalized on their top surface with a single-layer of molecules. The silicon block is perforated on its lower part and a SWCNT inserted through the perforation. The SWCNT acts as a fluid conduit. When the pH in the environment surrounding the nano-valve changes, the functionalizing molecules may acquire a larger charge. This, in turn, gives rise to a larger electrostatic repulsion between the molecules and, subsequently, causes the cantilever to bend downward. If the action of the cantilever causes the SWCNT to deflect past the point of bucking, the fluid-flow through the SWCNT ceased and the nano-valve is in the "*off*" position, Fig. 1(b).

For the nano-valve to function as described above, the reduction in the electrostatic energy associated with an increase in the inter-molecular separation during cantilever bending has to be sufficiently large to compensate for the elastic energies stored in the cantilever nano-beam and in the nano-tube (up to and past the point of buckling of the SWCNT). For a given charge-level of the functionalizing molecules, the electrostatic energy reduction is governed by the molecular surface coverage (density) and the surface area of the top face of the block and the cantilever. For a fixed molecular surface density and a fixed value of the combined lengths of the silicon block and the cantilever, the nano-valve width becomes the sole design parameter controlling the functionality of the nano-valve.

2.2. Application of shell theory to SWCNTs

Following previous work e.g. [4], a SWCNT is treated within a continuum approach as a cylindrical thin-wall shell. The stretching and the bending stiffnesses of such a shell can be determined using ab initio or atomistic simulations of the stretching and the bending behavior of SWCNTs e.g. [4]. Using standard relations given below, the two stiffnesses can next be converted into the effective elastic moduli (the Young's modulus and the Poission's ratio) and the effective thickness of the SWCNT (shell wall).

Within an atomistic simulation framework within which bonding between the carbon atoms in a SWCNT is represented using a forcefield, all terms in the forcefield potential affect the resistance of a SWCNT to any mode of deformation. However, the stretching stiffness is generally dominated by the resistance of SWCNTs to C–C bond stretching and to C–C–C (two-bond) in-plane bond-angle changes. Within the condensed-phased optimized molecular potential for atomistic simulation studies (COMPASS) forcefield [11], for example, these two forcefield terms are responsible for over 95% of the contribution to the stretching resistance. Likewise, the bending stiffness is mainly a measure of the resistance to C–C–C (two-bond) in-plane bond-angle, C–C–C–C dihedral torsion-angle and $\begin{matrix}\mathbf{C}\\ \mathbf{C}\end{matrix}>\mathbf{C}-\mathbf{C}$ out-of-plane inversion-angle changes.

Following the recommendation of Pantano et al. [4], representative values for the stretching stiffness, $C = 59.36\,\text{eV/atom} = 400.4\,\text{J/m}^2$, and for the bending stiffness, $D = 2.886\,\text{eV Å}^2\text{/atom} = 1.765 \times 10^{-19}\,\text{J}$ are used. The effective SWCNT wall Young's modulus, E_{wall}, and the effective SWCNT wall thickness, t_{wall}, are computed from the following relations:

$$C = E_{\text{wall}} t_{\text{wall}} \Omega \tag{1}$$

and

$$D = \frac{t_{\text{wall}}^3 E_{\text{wall}} \Omega}{12(1 - \nu_{\text{wall}}^2)} \tag{2}$$

as $E_{\text{wall}} = 4.84\,\text{TPa}$ and $t_{\text{wall}} = 0.075\,\text{nm}$, where $\Omega = 0.0262\,\text{nm}^2\text{/atom}$ is the surface area of the SWCNT wall allocated to a carbon atom, and $\nu_{\text{wall}} = 0.19$ is the SWCNT wall Poisson's ratio (set equal to that in a graphene sheet).

The SWCNT wall (i.e. the cylindrical shell wall) is discretized within the finite element framework used in the present work using four-node doubly curved shell elements, which allow transverse shear deformation. These elements are suitable for modeling the SWCNT wall using a continuum elastic shell model, which accounts for geometrical nonlinearities (critical for modeling the onset of buckling in the SWCNT). The reference surface of a (SWCNT wall) shell is defined in terms of the shell element nodal coordinates and the normal definitions. The shell's degrees of freedom including all kinematic quantities are all referred to such a reference surface.

2.3. Development of special interaction elements

To further include atomic-level effects into the present continuum-level analysis, van der Waals interactions between neighboring surfaces must be taken into account. Specifically, the van der Waals interactions between different sections of the internal surface of a SWCNT must be considered, since such interactions affect the post-buckling behavior and the reversibility of large-scale deformation in a SWCNT. In addition, the van der Waals interactions between the tip of the silicon cantilever nano-beam and the SWCNT fluid conduit control the transfer of the force from the nano-beam to the SWCNT, and, hence, must be taken into account.

The van der Waals interactions within a SWCNT are modeled using the following Lennard–Jones-based pressure/interlayer distance relation [4]:

$$P_{\text{C-C}} = \frac{\psi}{6}\left[\left(\frac{d_0}{\alpha}\right)^{10} - \left(\frac{d_0}{\alpha}\right)^{4}\right] \tag{3}$$

where P_{C-C} is the carbon–carbon interlayer contact pressure, α the interlayer distance, $d_0 = 0.34$ nm, the equilibrium graphene inter plane distance and $\psi = 36.5$ GPa.

To obtain a similar pressure/interlayer distance relation for the nano-beam/SWCNT interactions, a short molecular mechanics simulation analysis is carried out using the Accelrys' molecular modeling program, Discover [5], and the COMPASS forcefield potential [6]. Since the silicon block and the cantilever beam used in the present work have a cubic (0 0 1) orientation, a computational domain is constructed, which consists of one (0 0 1) silicon-plane and one graphene plane. The in-plane size of the computational domain in terms of the number of silicon lattice parameters used is seven by nine. The size of the corresponding graphene sheet was different by 0.9 and 0.7% in the x- and y-direction from those of the silicon-plane (0 0 1). To eliminate this difference, equal-magnitude/opposite-sign strains are applied, respectively, to the silicon and the graphene sheets, in both directions. The periodic boundary conditions are next applied in the x- and y-direction. The initial inter planar distance was then set to 0.8 nm and reduced repeatedly in decrements of 0.01 nm. At each value of the inter planar spacing, the interaction energy of the two planes is computed. The interaction energy is defined as a difference between a sum of the potential energies of the two planes at an infinite distance and the energy of the computational domain containing the two planes at a finite distance. The results of this calculation, as provided in Fig. 2(a), are fitted to the following functional form:

$$E_{\text{int}} = C\left[\frac{n}{m}\left(\frac{d_0}{\alpha}\right)^m - \left(\frac{d_0}{\alpha}\right)^n\right] \tag{4}$$

where m and $n < m$ are positive integers, and C is a positive proportionality constant.

The Levenberg–Marquart method for non-linear parameter estimation is next used to determine the unknown parameters: m, n, C and d_0 in Eq. (4). The fitting procedure yielded the following optimal values for the model parameters: $m = 7$, $n = 4$, $C = 0.6539$ J/m^2 and $d_0 = 0.364$ nm. The results of the fitting procedure are also displayed in Fig. 2(a). It is seen that Eq. (4) can quite successfully account for the interaction energy/inter planar spacing relation obtained using atomistic simulations.

Eq. (4) is next used along with the values of the optimal parameters to define the pressure/interlayer distance as:

$$P_{\text{Si-C}} = -\frac{\mathrm{d}E_{\text{int}}}{\mathrm{d}\alpha} = -\frac{Cn}{d_0}\left[\left(\frac{d_0}{\alpha}\right)^{m+1} - \left(\frac{d_0}{\alpha}\right)^{n+1}\right] \tag{5}$$

where $P_{\text{Si-C}}$ in the Si(0 0 1)/graphene interlayer contact pressure.

The pressure/interlayer-spacing relations given by Eqs. (3) and (5) are implemented in the ABAQUS user subroutine UINTER [7], which enables the user to specify the constitutive interactions between two deforming surfaces (a master and a slave surface). The subroutine is called for each slave node at each time increment during the finite element analysis to compute the tractions at such nodes based on the increments in their relative position with respect to the master surface. The normal tractions can be either positive (indicates surfaces repulsion) or negative (denotes surfaces attractive). In addition to computing the nodal traction, the UINTER subroutine is used to compute the corresponding Jacobian to help to accelerate convergence of the computational algorithm.

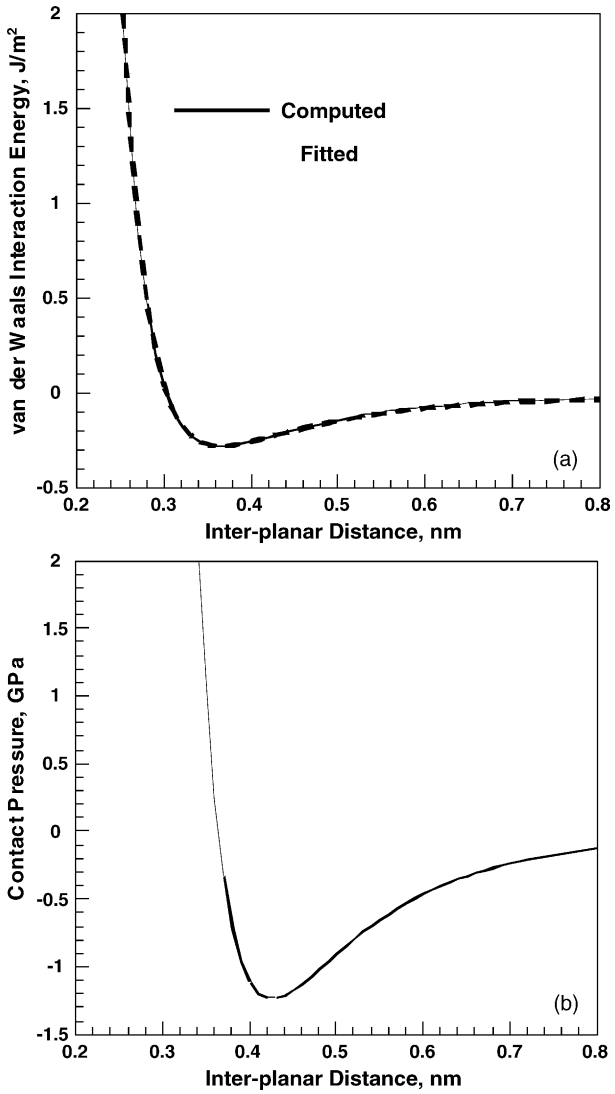

Fig. 2. Variation of: (a) the Si(0 0 1)/graphene interaction energy and (b) the contact pressure with the inter planar separation.

2.4. Evaluation of the monolayer electrostatic energy and force

The electrostatic energy and force for a functionalizing single-layer can be evaluated by placing charged particles at the positions on the top face of the silicon block and cantilever nano-beam, where the charged functional groups of the functionalizing monolayer would be located during bending. Such a procedure yields a functional form between the

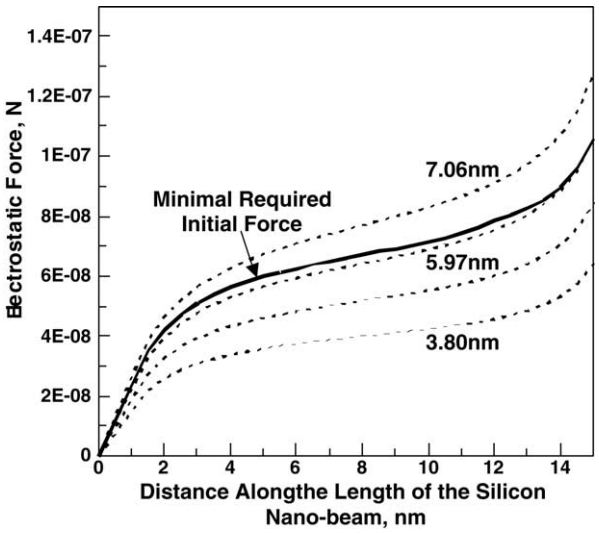

Fig. 3. Variations of the initial nodal forces for different nano-valve widths (dashed lines) and the initial minimal requires nodal forces (solid line) along the length of the cantilever nano-beam (measured from the fixed end of the nano-beam).

total electrostatic energy or the electrostatic forces acting on each charged particles at a given level of bending curvature of the cantilever. Ideally, one would like to use such forces within a static finite element analysis like the one used in the present work (described in the next section). However, the finite element program ABAQUS [7] used in the present work does not allow the applied force to be varied during the simulation run, i.e. only time-independent concentrated or distributed forces can be used. To overcome this limitation, the procedure described below was utilized, which involves the following steps:

(a) A cantilever nano-beam with a sufficient width is first selected to ensure that the electrostatic forces acting between the charged particles are sufficiently large to give rise to the nano-tube buckling. For a give molecular surface coverage and particle charges, the force on each charged particle, i, due to its interaction with all other particles, j, is next computed using the following equation:

$$\mathbf{F}_i = -\frac{1}{4\pi\varepsilon_0}\sum_j \frac{q_i q_j}{r_{ij}^2}\mathbf{r}_{ij} \quad (j \neq i) \tag{6}$$

where q_i and q_j are the charge of particles i and j, r_{ij} the i–j inter distance, $\mathbf{r}_{ij}$ the unit vector point along the direction connecting particle i to j, ε_0 the permittivity of free space and bold fonts are used to denote vector quantities.
Since the plane-strain boundary conditions are applied to the cantilever nano-beam in the width direction, the forces acting on all atoms at a given location along the cantilever length (i.e. at a given x-coordinate) are first summed, then divided by 2 and finally assign to each of the two nodes at a given x-location at the top face of the cantilever nano-beam Fig. 3.

(b) Once such forces are computed for all the nodes at the top face of the cantilever nano-beam, a finite element analysis is carried out until the onset of SWCNT buckling. At that point, the coordinates of all the nodes at the top face of the cantilever nano-beam are determined and the forces acting on each corresponding charged particle calculated using Eq. (6). Since the charged particles are separated further apart in the deformed cantilever configuration, the forces computed are lower in magnitude relative to their counterparts in the original nano-tube configuration.

(c) Next, it is imposed that the work done by each node under the condition of a constant force between the initial and the final configuration (as encountered during a finite element method run) is identical to that which would be done, if the force acting on that node were allowed to vary with the nano-beam curvature. This requirement and the fact that the electrostatic force decreases as $1/r_{ij}^2$ during cantilever bending were then used to determine the appropriate initial force, which should act on each of the nodes. A variation of such a minimum required initial force acting on the nodes with a distance along the cantilever nano-beam for a nano-valve with a silicon block length of 40, the cantilever nano-beam length of 30 and the width of 14 (all in terms of the number of silicon lattice parameters) is shown in Fig. 3, curve labeled “minimal required initial force”.

(d) The variation of the force acting on the individual nodes along the nano-beam length in the initial configuration is next generated using the procedure described in part (a) for several nano-beam widths. The nano-beam widths are incremented by an integer number of silicon lattice parameters. The smallest nano-beam width, which satisfies the condition that the force acting at any node in the initial configuration is greater than the minimal required initial force is deemed as the minimal acceptable cantilever beam width.

2.5. Initial internal state within the SWCNT

As pointed out by several research groups e.g. [8,9], the SWCNTs contain an internal stress due to their curvature. Pantano et al. [4] observed that such internal stress can play a major role in the ability of a SWCNT to recover large localized strains and, hence, must be taken into account in the present case, where such strain reversibility is critical aspect of the “*on/off*” switching behavior of the fluid-flow nano-valve. To compute the initial circumferential internal stress within the SWCNT, σ_θ, the rolling (strain) energy of a single graphene sheet:

$$U_{\mathrm{R}} = \frac{D}{2R_{\mathrm{SWCNT}}^2} = \frac{1}{2}D\kappa_{\mathrm{wall}}^2 = \frac{t_{\mathrm{wall}}^3 E_{\mathrm{wall}}}{24(1-\nu_{\mathrm{wall}}^2)}\kappa_{\mathrm{wall}}^2 \tag{7}$$

is differentiated with respect to nano-tube radius, R_{SWCNT}, to get:

$$\sigma_\theta = -\frac{t_{wall}^3 E_{wall}}{12(1-\nu_{wall}^2)} \frac{1}{R_{SWCNT}^3} \quad (8)$$

where $\kappa_{wall} = 1/R_{SWCNT}$ is the SWCNT wall curvature.

The circumferential internal stress given by Eq. (8) is incorporated into the ABAQUS subroutine SIGINI in order to specify the initial stress state in the nano-tube (shell) wall.

2.6. Finite element analysis

While many commercial finite element codes are capable of handling geometrically non-linear small-strain/large-rotation shell (used to represent the SWCNTs) and brick (used to represent silicon cantilever nano-beam) elements, ABAQUS standard [7] is chosen in the present investigation, as indicated earlier, since it contains user subroutines for implementation of the van der Waals interactions and the initial internal stress state in the nano-tube.

A schematic representation of the finite element model is shown in Fig. 4 along with the appropriate initial and boundary (loading) condition. The SWCNT is represented using four-node doubly curved reduced-integration elements *S4R* with hourglass control. The silicon cantilever is represented using eight-node brick element *C3D8* ABAQUS elements. Following Pantano et al. [4], the *S4R* shell elements are selected to be approximately square in shape and to have a side length around 0.24 nm, the height of the hexagonal cell in the graphene plane. The size of the *C3D8* elements in the *x*- and *y*-direction is chosen to nearly match that of the shell elements. Almost identical results of the finite element analyses are obtained using elements, which are larger or smaller by a factor of , suggesting that a mesh-size invariance condition has been attained.

The SWCNT material is modeled as an elastically isotropic material with E_{wall} and ν_{wall} given in Section 2.2. The silicon material is also modeled as an isotropic linearly elastic material with $E_{beam} = 76.7$ GPa and $\nu_{beam} = 0.26$. These values were obtained by fitting the bending energy results obtained using atomic-level bending simulations to a standard bending energy/bending curvature relation [3].

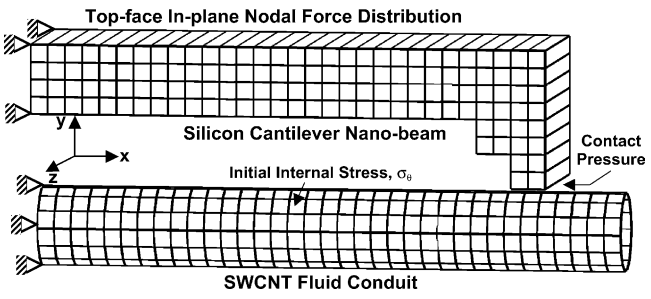

Fig. 4. The formulation of the finite element boundary value problem analyzed in the present work.

3. Results and discussion

3.1. Validation of the present finite element method

For the silicon cantilever beam-based fluid-flow nano-valve analyzed in the present work to be functional, the diameter of the SWCNT fluid conduit must be large enough to enable a free passage of the molecules, which as in the case of organic substances or drugs, may have a large size. A large diameter SWCNT, however, requires a large silicon block, a large cantilever nano-beam and, thus, a large number of functionalizing molecules in the top face monolayer. Consequently, the number of particles in the device may become prohibitively large for the problem to be analyzed using molecular modeling. That is, the reason why a finite element method-based approach, which does not suffer from the similar limitations, is developed in the present work. However, the molecular modeling approach is intrinsically more accurate and reliable than its finite element counterpart and, hence, one must develop a procedure for validating the latter.

The procedure used in the present work to validate the finite element-based approach involves finding the solution to the same problem by using both a more accurate molecular modeling method and the less accurate finite element method-based approach presented in Section 2.6. Due to the limitations of the molecular modeling approach described above, a nano-valve of a smaller size than the one, which could function as a regulator for the flow of organic/drug molecules are analyzed. Specifically, a (8, 8) SWCNT (the nano-tube radius = 0.54 nm, the nano-tube length = 12.0 nm) is selected as the flow conduit and the lengths of the silicon block and the cantilever length are both set to 5 nm.

Next, the procedure described in Sections 2.4 and 3.2 is utilized to determine the minimal required silicon block/cantilever width, which gives rise to nano-tube buckling. This width was found to be 14 silicon lattice parameters, and is in very good agreement with its counterpart (13 silicon lattice parameters) determined using molecular mechanics simulations. The details of the molecular modeling simulations can be found elsewhere [10].

To further validate the finite element-based approach developed in the present work, a comparison is made in Fig. 5 between the total strain energies (the strain energies stored in the silicon cantilever nano-beam and the SWCNT) as a function of the cantilever curvature obtained using the present approach and molecular modeling. It is seen that the agreement between the two sets of results is good both relative to the curvature dependence of the strain energy and relative to the value of critical curvature, at which nano-tube buckling occurs.

The results presented in the present section are encouraging and suggests that the present finite element-based approach is a valuable alternative for modeling the performance of functionalised beam/carbon-nano-tube-based nano-devices.

3.2. Optimization of the nano-valve design

In this section, the finite element-based method developed in Section 2.6 is used to identify the optimal geometry of the nano-valve under consideration.

The first step toward designing the nano-valve is to select the appropriate SWCNT. As explained earlier, it is desirable to have a SWCNT with a sufficiently large diameter to enable an easy passage of the molecules, when the nano-valve is in the open position. However, previous molecular mechanics studies e.g. [10] have shown that SWCNTs can maintain a stable circular cross-section only up to a radius of approximately 3 nm. In the (*n*, *n*) arm-chair family of SWCNTs, the nano-tube with the largest radius capable of retaining a stable circular cross-section is found to be a (15, 15) SWCNT. In the arm-chair SWCNTs with a larger radius, the circular cross-section subjected to compression (in a direction normal to the nano-tube axis) may collapse to a shape consisting of a central region, in which the opposite walls of the nano-tube are nearly parallel to each other and at a distance comparable to the basal-plane spacing in graphite. The side portions of the cross-section consist of nearly circular regions with a radius of approximately 0.75 nm, which appears independent of the value of the chiral number $n > 15$ in the arm-chair SWCNTs. In the arm-chair family of SWCNTs between (16, 16) and (45, 45), either the circular or the collapsed cross-sections may be stable depending on the magnitude of the compression applied to the SWCNT with an initial circular cross-section. At low-levels of the compression, the circular cross-section is stable while at large-levels of the compression, the collapsed cross-section is more stable. In the arm-chair family of SWCNTs, nano-tubes with the chirality index $n > 45$, only the collapsed cross-section becomes stable. In other words, no energy barrier exist in the configurational space exist between the circular and collapsed cross-sections of the SWCNTs.

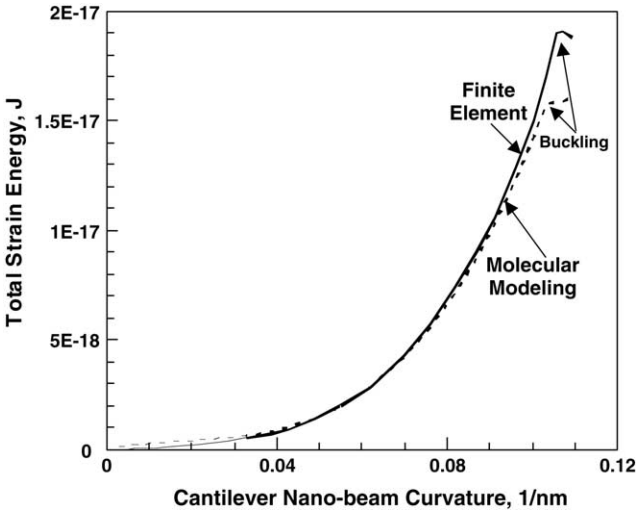

Fig. 5. Variation of the total strain energy with the silicon nano-beam curvature.

A stability analysis for the circular cross-section of the SWCNTs is carried out in this work using the present finite element formulation. The results obtained show that, for the arm-chair family of SWCNTs, the nano-tubes with the chirality index $n < 17$ have a stable cross-sectional shape, while those with $n > 43$ are stable in the collapsed cross-sectional shape. For the SWCNTs with an intermediate value of *n*, either of the two cross-sections can be stable, depending on the type and magnitude of the perturbation applied to the nano-tube with a circular cross-section. The observed good agreement between the results of the atomic-level and the continuum-level analyses of stability of the circular cross-section in the SWCNTs suggests the finite element formulation proposed in the present work can realistically represent deformation behavior of the SWCNTs.

A loss of the circular cross-section is not acceptable in the present case, since it prevents the passage of large molecules and interferes with the normal "*on/off*" switching of the nano-valve. Consequently, a (17, 17) SWCNT with a radius of 1.15 nm is selected. Such SWCNT offers a compromise between a desirable large cross-section area, required stability of the SWCNT circular cross-section and the SWCNT's ability to recover a large (post-buckling) localized strain. The length of the (17,17) SWCNT is next arbitrarily set to ∼50 nm. To match the length of the SWCNT, the lengths of the silicon block and the cantilever nano-beam are each next set to ∼20 nm. Furthermore, a sufficiently large width for the silicon block/cantilever nano-beam of ∼108.6 nm (20 silicon lattice parameters) is selected, so that, when the charge on each functional group of the monolayer molecules is chosen arbitrarily as 0.3*e* (*e* is the unit electrical charge), SWCNT buckling can take place during cantilever actuation.

Using the aforementioned values for the nano-valve components, a finite element simulation run of the nano-valve closing operation due to cantilever actuation is carried out up to the point of nano-tube buckling. The morphology of the nano-valve at the onset of SWCNT buckling is shown in Fig. 5. Following the procedure presented in Section 2.4, the distribution of the initial required nodal forces along the cantilever length is next determined. This distribution is shown in Fig. 4, the solid curve labeled "minimal required initial force". Next, a set of dashed curves displayed in Fig. 4 is generated, each corresponding to the initial distribution of the nodal forces along the cantilever length in a nano-valve of a given width. To meet the requirements that the initial nodal force is higher than the required minimal force for each node and that the nano-valve width is minimal, the lowest dashed curve, which is above the solid curve (the one labeled "minimal required initial force") is selected to identify the minimal required nano-valve width (∼7.06 nm = 13 silicon lattice parameters).

Once the minimal required width of the nano-valve is determined, the finite element method is applied again for the redesigned nano-valve to verify that the device is indeed functional. Furthermore, a device with a width of 6.52 nm (i.e. one silicon lattice parameter smaller width than the minimal

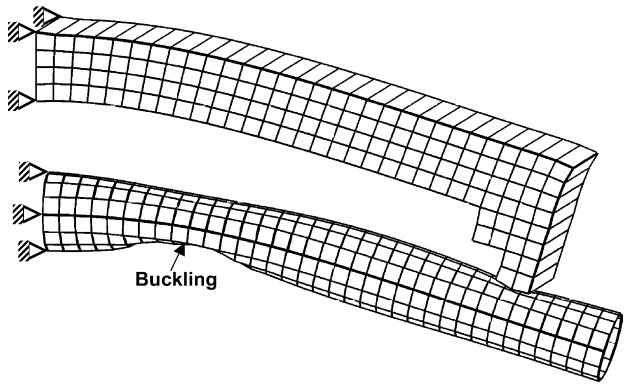

Fig. 6. An example of the nano-valve configuration at the onset of SWCNT buckling.

required width) is also analyzed using the finite element method to verify that such a nano-device would not function, since the reduction of the electrostatic energy during cantilever nano-beam bending is not sufficient to compensate for the elastic strain energy build-up in the nano-beam and in the SWCNT.

The geometrically optimized nano-valve described above contains 94,710 atoms including 518 functionalized groups in the top face monolayer. Molecular modeling, for the reasons presented in Section 1, is not suitable for the analysis of a device with this many of atoms. Solares et al. [3] proposed a hybrid method within which the individual components of the nano-device are modeled using molecular modeling, while the analysis of the device as a whole is carried out using a classical mechanical design approach. We applied the approach of Solares et al. [3] to the geometrically optimized nano-valve design. We found out that the present design would be also functional according to the method of Solares et al. [3]. However, the method of Solares et al. [3] also predicts that as a device with a width smaller by two silicon lattice parameters than the minimal required width would also be functional in sharp contrast with the predictions of present finite element approach. Since both the hybrid approach of Solares et al. [3] and the present finite element approach utilize atomic-level derived properties of the nano-valve components, the discrepancy between the two approaches can be explained by recognizing that within the present finite element approach, the interactions between nano-valve components are taken into account, while such interactions are not considered in the approach of Solares et al. [3]. An example of the effect of the interaction between the cantilever beam and the SWCNT fluid-flow conduit is seen in Fig. 6, where the nanotube undergoes a localized dimpling deformation at the point of contact with the cantilever tip. Such deformation is associated with an additional strain energy, which is accounted for in the present work but not in the approach of Solares et al. [3].

3.3. Design considerations for an "in-line" nano-valve

The nano-valve configuration shown in Fig. 1 is generally referred to as "free-end" design, in which the nano-tube

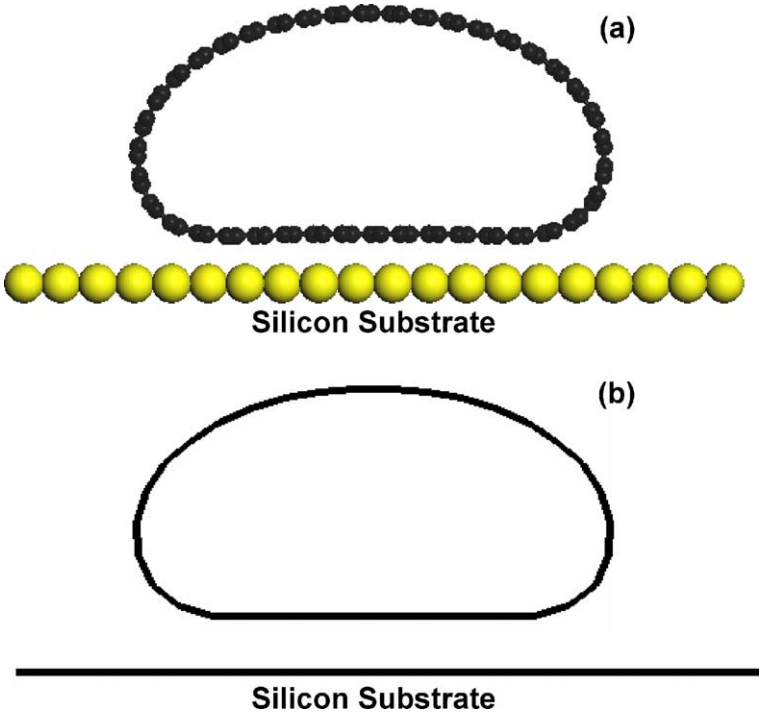

Fig. 7. A comparison of the cross-sections of infinitely long (20,20) arm-chair SWCNTs interacting with a (1 0 0) silicon substrate obtained using: (a) an atomic-level energy minimization analysis and (b) a finite element perturbation analysis.

fluid-flow conduit can freely bend under the effect of the cantilever beam until the point of buckling is attained. There is an alternative design of the nano-valve generally referred to as an "in-line" design [3]. In this design of the nano-valve, a SWCNT fluid-flow conduit is positioned on the top of a rigid silicon single-crystal substitute (beam). Consequently, bending of the silicon cantilever during the closing operation of the nano-valve causes local crimping of the nano-tube, which stops the flow of the fluid. Since the SWCNT lies on the silicon substitute, its atoms interact with those of the substitute, causing a change in the SWCNT cross-section. A severe departure of the SWCNT cross-section from a circular shape, when the nano-valve is in the open position is generally not desirable, since it may interfere with the flow of the fluid. In this section, we conducted a test of the present finite element method to determine if this method can correctly account for the SWCNT/substrate interaction induced loss of the SWCNT circular cross-section.

A comparison of the atomic-level and the finite element method results of the optimal cross-section shape of an infinitely long (20, 20) SWCNT in contact with a silicon substitute is given in Fig. 7(a) and (b). A fairly good agreement between the two sets of results shown in Fig. 7(a) and (b) suggest that the present finite element approach can be used for the design of an in-line type of the nano-valve. A detailed design analysis of an in-line nano-valve will be carried out in our future work.

4. Conclusions

Based on the results obtained in the present work, the following main conclusions can be drawn:

1. A finite element method-based procedure for the analysis of nano-size devices, in which doubly curved shell elements are used to represent the SWCNT wall yield the results, which is quite comparable to their molecular modeling counterparts.
2. The use of a continuum-based procedure, such as the one developed in the present work, enables the analysis of nano-size devices, for which a purely molecular analysis would be either impractical or impossible.

Acknowledgements

The material presented in this paper is based on work supported by the U.S. Army Grant Number DAAD19-01-1-0661. The authors are indebted to Dr. Bonnie Gersten, Dr. Fred Stanton and Dr. William DeRosset of ARL for the support and a continuing interest in the present work.

References

[1] J. Fritz, M.K. Baller, H.P. Lang, T. Strunz, E. Meyer, H.-J. Guntherodt, E. Delamarche, Ch. Gerber, J.K. Gimzewski, Langmuir 16 (2000) 9694–9711.
[2] R. Berger, E. Delamarche, H.P. Lang, Ch. Gerber, J.K. Gimzewski, E. Meyer, H.-J. Güntherodt, Appl. Phys. A 66 (1998) S55–S59.
[3] S. Solares, M. Blanco, W.A. Goddard III, Nanotechnology 15 (2004) 1405–1415.
[4] A. Pantano, M.C. Boyce, D.M. Parks, J. Mech. Phys. Solids 52 (2004) 789–821.
[5] http://www.accelrys.com/mstudio/msmodeling/discover.html.
[6] H. Sun, J. Phys. Chem. B 102 (1998) 7338.
[7] ABAQUS Manuals 6.3, ABAQUS, Inc., Pawtucket, RI, 2002.
[8] B. Yakobson, P. Avouris, in: M.S. Dresselhaus, et al. (Eds.), Carbon Nano-tubes, Springer, Heidelberg, 2001, p. 287.
[9] G. Gao, T. Cagin, W.A. Goddard III, Nanotechnology 9 (1998) 184–191.
[10] G. Cao, Multi-length scale modeling of processing, properties and performance of carbon nano-tubes and nano-devices, Ph.D. Thesis, Clemson University, 2004.
[11] H. Sun, P. Ren, J.R. Fried, Comput. Theor. Polym. Sci. 8 (1/2) (1998) 229–249.